TESCAN

PERFORMANCE IN NANOSPACE

GAIA3

Extraordinary Ultra-High Resolution imaging and extremely precise nanoengineering

GAIA3 is the ideal platform for performing the most challenging nanoengineering applications that require ultimate precision and demanding capabilities for microanalysis. Preparation of high-quality ultra-thin TEM lamellae, delayering processes in technology nodes, precise nanopatterning and high-resolution 3D reconstructions are just some of the applications in which GAIA3 excels.

- **Triglav™ - newly designed Ultra-High Resolution (UHR) electron column equipped with the TriLens™ objective and an advanced detection system**
  - Unique combination of a **three-lens objective and cross-over-free mode**
  - Advanced and variable detection system for simultaneous acquisition of various signals
  - Sub-nanometre resolution: **0.7 nm at 15 keV**
  - Ultimate ultra-high resolution: **1 nm at 1 keV**
  - Angle-selective BSE detection for maximum topographical and elemental contrast at low energies
  - Real-time **In-Flight Beam Tracing™** for performance and beam optimisation
  - Traditional TESCAN Wide Field Optics™ design offering a variety of working and display modes
  - Efficient thermal power dissipation for excellent electron column stability
  - New Schottky FE gun now enables **beam currents up to 400 nA and rapid beam energy changes**
  - Ideal solution for inspecting the latest technology nodes in advanced failure analysis processes
  - Ideal for imaging delicate biological specimens
  - Imaging of magnetic samples possible
  - Optimised column geometry makes analysis (SEM inspection and FIB nanomachining) of up to 8" wafers possible
  - Unique live stereoscopic imaging using **3D Beam Technology**
  - User-friendly, sophisticated SW modules and automatic procedures

- **Cobra FIB column: High-performance Ga FIB column for ultimate precision in nanoengineering**
  - **Top level technology** in terms of resolution for both milling and imaging
  - Cobra FIB column guarantees **the shortest time to result** in cross-sectioning and TEM sample preparation
  - Ultimate FIB resolution of **< 2.5 nm**
  - FIB-SEM tomography for **high-resolution 3D microstructural analysis**
  - Ideal for **3D ultra-structural studies of biological specimens** such as tissue and whole cells
  - **Excellent performance at low kV** ideal for polishing ultra-thin lamellae and for reducing amorphous layers

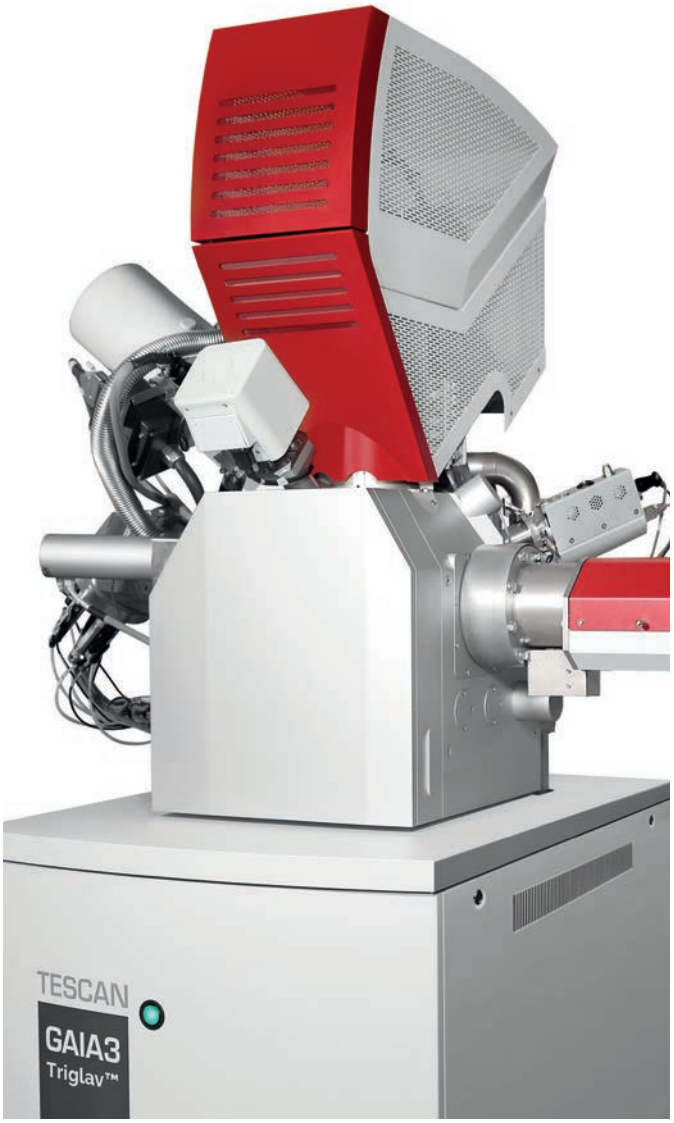

These features make GAIA3 the ideal instrument for applications in which imaging at low beam energies is a requirement to preserve delicate structures in samples that can get easily damaged by the electron beam such as low-k dielectric materials, photoresists or uncoated biological specimens. In terms of sample modification, GAIA3 represents the most suitable solution for challenging nanomachining and nanofabrication.

Triglav™
Experience ultimate resolution

The new TESCAN SEM column Triglav™ delivers a unique combination of immersion optics and crossover-free mode for UHR imaging at low energies. The single-pole type objective lens creates a magnetic field around the sample and dramatically decreases optical aberrations. Avoiding any crossover in the column reduces the Boersch effect and further optimizes the electron beam to yield superior resolution. Surface details of the specimen can be captured more reliably than ever before. For analysis, the TriLens™ technology improves resolution in the magnetic-field-free mode.

Key benefits

- **TriLens™:** Objective based on the advantageous complementarity of three lenses that enables multiple imaging modes
- Unique combination of UH-resolution lens with crossover free mode for superb ultra-high resolution: **1 nm at 1 keV**
- **TriSE™:** Three SE detectors to capture the finest surface details
- **TriBE™:** Three BSE detectors for angle-selective compositional contrast
- **EquiPower™:** Excellent column stability ideal for time-consuming applications such as FIB-SEM tomography

In-Beam SE	**0.7 nm at 15 keV**
SE (BDM)	**1.0 nm at 1 keV**
STEM	**0.7 nm at 30 keV**

TriLens™ - Three lenses, various imaging modes

The TriLens™ objective system is based on the advantageous complementarity of three objective lenses: an UH-resolution lens (60° immersion lens), an Analytical lens and an Intermediate lens (IML). The combination of these lenses results in different working imaging modes.

UH-RESOLUTION mode

This mode is achieved by the unique combination of immersion optics and **crossover-free mode** for **ultra-high resolution** imaging at low energies. Avoiding any crossover in the column reduces the Boersch effect and further optimizes the electron beam to yield superior resolution of 1 nm at 1 keV. UHR is ideal for failure analysis in semiconductors, research and characterisation of nanomaterials, non-conductive and very sensitive samples.

ANALYSIS mode

This mode is implemented by means of the Analytical lens. It is well suited for analysis such as EDS and EBSD, as well as simultaneous SEM imaging during FIB operations such as cross-sectioning and FIB-SEM tomography. High-quality imaging of highly topographic magnetic specimens is possible.

DEPTH mode

The UH-resolution lens can be used in combination with the IML lens which allows for increasing the probe current while maintaining excellent resolution and enabling large depth of focus. This further extends the analytical capabilities and enables imaging of sensitive samples with high topography.

OVERVIEW mode

The IML enables a wide field of view.

1

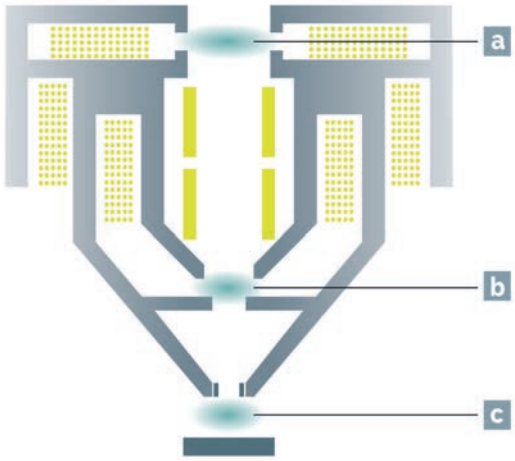

Fig. 1: The **TriLens™** objective system. **(a)** IML **(b)** Analytical lens **(c)** UH-resolution lens

2

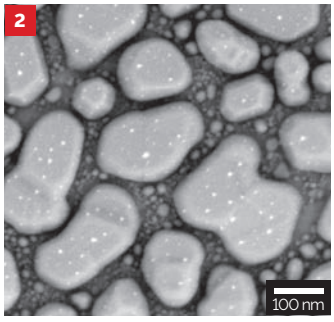

IMAGING MODES

- **UH-RESOLUTION** for the best resolution
- **ANALYSIS** for analytical techniques
- **DEPTH** for higher depth of focus
- **OVERVIEW** for large field of view

Fig. 2: Resolution test: gold particles on carbon imaged at 50 eV with the SE (BDM) detector in the UH-RESOLUTION mode.

TriSE™ + TriBE™ - Universal detection system

See even more with the advanced **Triglav™** detection system involving several high-efficiency detectors in the column as well as in the chamber for secondary, back-scattered and transmitted electrons.

TriSE™ – triple SE detection – gives a nearly noise-free comprehensive description of sample topography and allows capturing the finest surface details. Each working mode – whether for ultra-high resolution, analysis or beam deceleration – is equipped with a dedicated SE detector placed in an ideal position with appropriate signal guiding electrodes.

TriBE™ – triple BSE detection – is used to distinguish BSE take-off angles and provides comprehensive information about material composition. A retractable In-Chamber BSE detector placed between the sample and the pole-piece provides both topographic and compositional contrast (from wide-angle electrons) suitable for observation of low-contrast samples. Mid-Angle BSE detector inside the column allows low-noise volume compositional mapping. In-Beam BSE detector captures true compositional information due to pure surface material contrast from axial backscattered electrons.

3

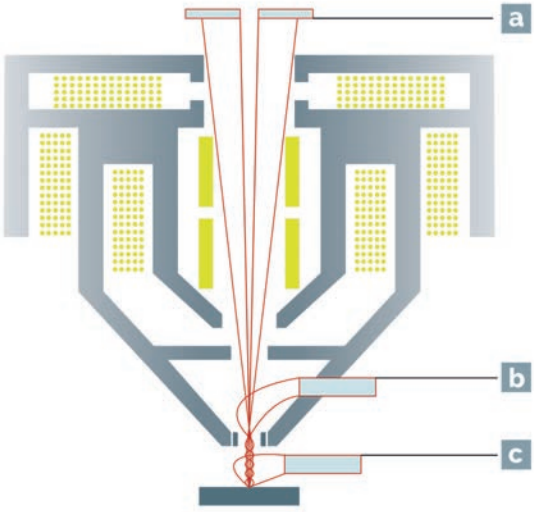

Fig. 3: See true sample topography. **(a)** BDM, **(b)** UH RESOLUTION and **(c)** ANALYSIS modes have their own dedicated detectors in ideal positions to capture fine surface details of the specimen.

4

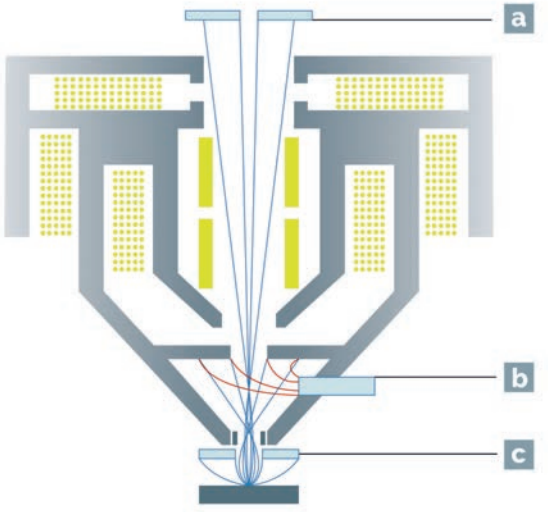

Fig. 4: The sophisticated geometry of detector arrangement enables distinguishing BSE take-off angles. **(a)** In-Beam BSE captures axial BSEs for pure surface Z contrast. **(b)** Mid-Angle BSE gives volume Z contrast and **(c)** In-Chamber BSE detector provides topographic and compositional contrast.

- **TriSE™ – Unique Triple SE detection system**
  - **In-Chamber SE**
    For topographical contrast.
  - **In-Beam SE**
    For ultra-high resolution and maximum surface sensitivity.
  - **SE (BDM)**
    For ultimate imaging in the beam deceleration mode (BDM).

- **TriBE™ - Unique Triple BSE detection system**
  - **In-Chamber BSE (retractable)**
    For wide-angle BSE detection which provides mainly topographical but also compositional contrast, especially suited for low-contrast samples (e.g. polished samples).
  - **Mid-angle BSE**
    For medium-angle BSE signal detection which is ideal for imaging at very small WD providing mainly compositional but also topographical contrast.
  - **In-Beam BSE**
    For axial BSE detection which provides pure surface material contrast and best suited for short WD.

The column excels throughout the entire range of accelerating voltages, however, the highlight is the ultimate resolution at low beam energies which makes this new column ideal for imaging beam-sensitive materials such as:

- **low-k dielectric materials**
- **photoresists**
- **nonconductive materials**
- **uncoated biological specimens**

In-Chamber SE

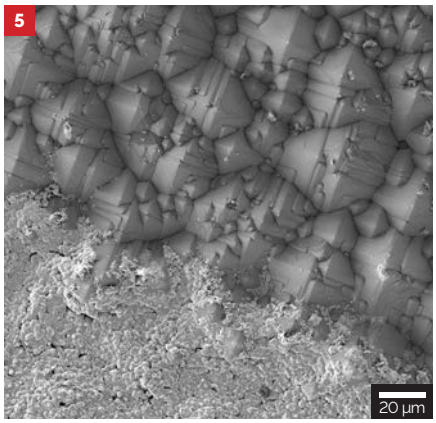

In-Beam SE

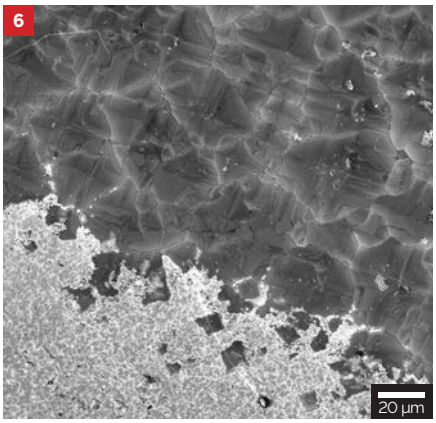

Fig. 5-9: SiN with Ag contact imaged at 5 keV with: **(5)** The In-Chamber SE detector which delivers excellent topographic contrast and is less sensitive to charging **(6)** The In-Beam SE detector for ultimate resolution **(7)** The In-Chamber BSE detector for collecting wide angle BSE giving topographic and material contrast **(8)** The Mid-Angle BSE detector for material contrast from the whole interaction volume **(9)** The In-Beam BSE detector for collecting axial BSE for material contrast of uppermost surface layers

In-Chamber BSE

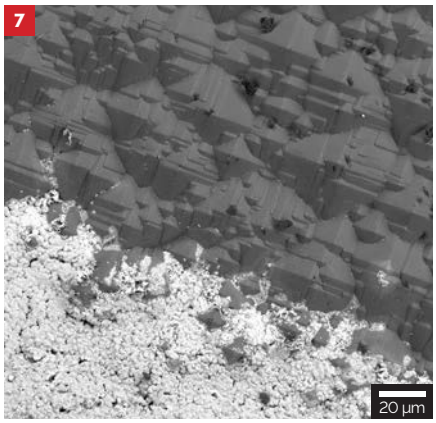

Mid-Angle BSE

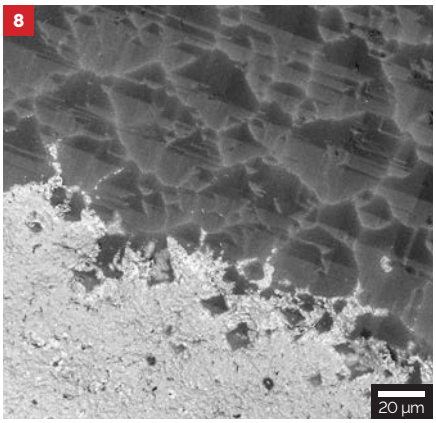

In-Beam BSE

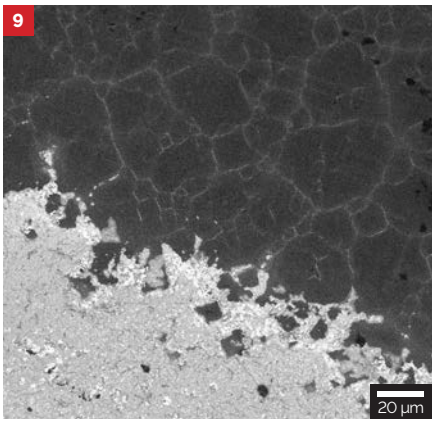

Beam Deceleration Mode

When the beam deceleration mode (BDM) is enabled, the detection system allows distinguishing between SE and BSE signals and therefore simultaneous acquisition of both. In this mode, ultimate resolution at low landing energies is achieved for maximum surface sensitivity and outstanding topographical and elemental contrast.

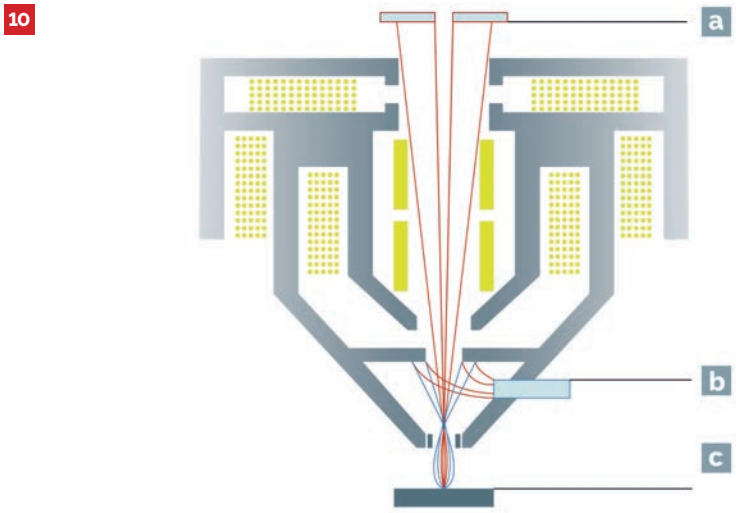

Fig. 10: The detection system allows simultaneous acquisition of SE and BSE signals in the beam deceleration mode (BDM). **(a)**. The SE (BDM) detector. **(b)**. BSE (BDM) detector. **(c)**. Biased sample.

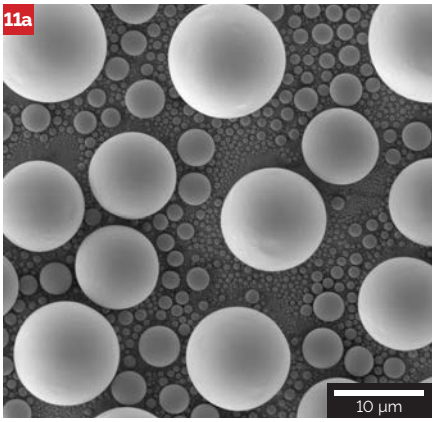

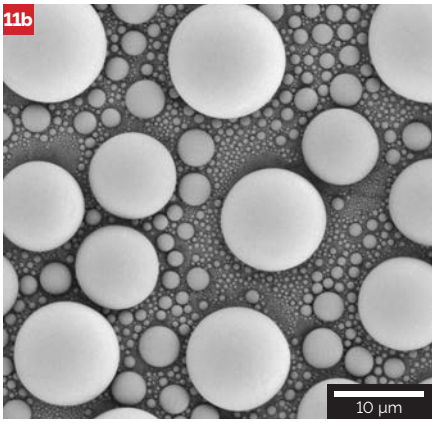

Fig. 11: Tin balls on carbon imaged in the BDM at 1 keV using the SE (BDM) detector **(a)** providing topographic information with typical edge effect and using BSE (BDM) detector **(b)** giving a compositional information.

Imaging at low and ultra-low energies for maximum surface sensitivity

The high-performance and ultimate resolution achieved by the Triglav™ column at low beam energies makes GAIA3 the ideal instrument for imaging any kind of beam sensitive samples such as delicate components in integrated circuits or non-conductive materials such as polymers, ceramics, etc. Low beam energies are essential for imaging biological specimens without conductive coatings.

This is an important requirement in order to resolve very fine structures in the surface of samples which in some cases can be affected by even the thinnest of coating layers. The interaction volume at low beam energies (~1 keV) is sufficiently small to achieve high spatial resolution. In addition, low beam energies can be very useful for imaging with enhanced contrast. Furthermore, BSE images at low beam energies are ideal for FIB-SEM tomography applications. In FIB-SEM tomography, the sample is sequentially FIB-sliced in thin layers (each a few tens of nanometres thick) followed by SEM-imaging. The BSE signal is used for image acquisition of each layer because it provides material contrast. At high energies, the BSE interaction volume is too large making it unsuitable for imaging such thin layers. Therefore, in order to achieve high-resolution FIB tomography the ability of imaging at low beam energies becomes crucial. TESCAN has designed a series of dedicated detectors optimised for operation in the low beam energy regime to ensure high signal collection yields resulting in maximum contrast.

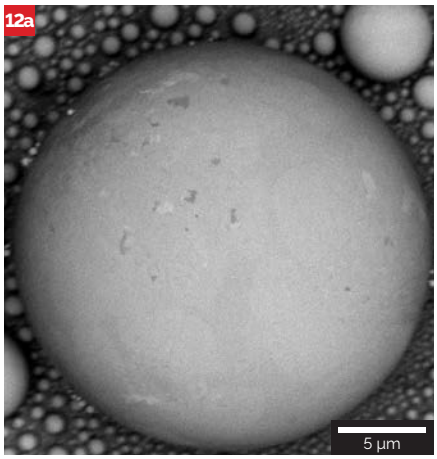

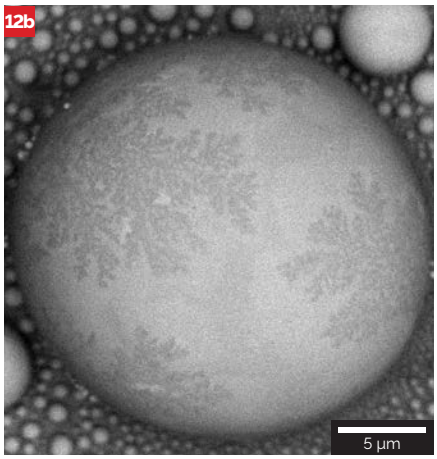

Fig. 12: Sn ball imaged at low beam energies with the LE-BSE detector. **(a)** At 1 keV **(b)** At 500 eV. Fine surface structure that remained hidden at 1 keV becomes visible at 500 eV.

■ Retractable Low-Energy BSE (LE-BSE) and Mid-Angle BSE detectors

These detectors are specially designed to significantly increase detection sensitivity at low energies, each of them aimed at different BSE take-off angles. The in-chamber LE-BSE detector collects electrons from wider angles while the in-column Mid-Angle BSE detector detects medium angles, in addition to the In-Beam BSE detector that collects axial electrons. Both LE-BSE and Mid-Angle BSE detectors are capable of operating over the entire range of the acceleration voltages, i.e. from 30 keV to down to 200 eV.

■ The In-Beam LE-BSE detector has a detection limit of 500 eV

This version is suitable for FIB-SEM tomography applications as it is protected from material deposition produced during FIB milling.Combining all detectors guarantees enhanced surface sensitivity and topographical contrast down to low energies.

■ Beam Deceleration Technology for imaging at low and ultra-low energies

Beam deceleration technology (BDT) consists of the beam deceleration mode (BDM) and high-performance In-Beam detectors for simultaneous SE and BSE signal detection in this mode. In the BDM, the energy of the electrons in the beam is decreased before they impact the surface of the specimen by means of a negative bias voltage which is applied to the sample stage. Ultra-low landing energies down to 50 eV (or 0 eV in manual control) are achievable. BDM enhances the performance of the electron column by reducing optical aberrations, thus allowing small spot sizes and high-resolution imaging at low energies. Low electron energies are advantageous for reducing charging effects in non-conductive samples as well as for imaging beam-sensitive specimens such as transistor layers in cross-sectioned integrated circuits for failure analysis, low-k dielectric materials and photoresists. BDM is especially suited for imaging biological specimens in their uncoated state at ultra-low beam energies without damaging the samples. In this mode, ultimate resolution at low landing energies is achieved for maximum surface sensitivity and outstanding topographical and material contrast.

Combining all TriSE™ and TriBE™ detectors guarantees enhanced surface sensitivity, topographical and material contrast down to low energies.

Achieve the ultimate in **nanomachining and nanofabrication**

GAIA3 features a state-of-the-art Ga ion source column with excellent performance: the Cobra column, the sharpest instrument for nanomachining capable of achieving a resolution of less than 2.5 nm which is ideal for challenging milling tasks that require ultimate precision.

A gas injection system (GIS) extends the analytical capabilities and thus the range of FIB-SEM applications. A GIS delivers different gas chemistry that reacts with the ion beam resulting in decomposition of the gas. Such process makes possible the deposition of conducting materials used for growing protective masks reducing surface charging effects during the preparation of cross-sections and TEM lamellae. Highly localised and controlled deposition can also be applied for circuit editing. In this regard, the ultimate FIB resolution achieved by GAIA3 allows challenging circuit edit in multi-layer 3D integrated circuits characterised by high density and thin layers thus making extreme precision - a must for successfully performing such editing tasks. In certain materials, milling rates can also be enhanced by using appropriate gas chemistry; for instance, XeF_2 to enhance the milling rate in silicon.
The combination of high-resolution SEM imaging with controlled etching allows the user to identify areas of interest on a sample and prepare site-specific TEM lamellae which are essential for failure root cause identification. The outstanding imaging and precise milling capabilities of GAIA3 make it the platform of choice for preparing ultra-thin lamella less than 15 nm thick which can then be in-situ analysed by means of the TESCAN STEM detectors at sub-nanometre resolutions. High-resolution FIB-SEM tomography is yet another of the highlighted applications; 3D sample reconstructions with a voxel size of just a few nanometres for maximum resolution is possible only with the extreme precision achieved by GAIA3's FIB column. The following table lists typical FIB tasks in different ion beam current ranges.

FIB milling optimisation essential kit

- **DrawBeam Advanced:** Shape correction for reducing redeposition artefacts, FIB end-point detection, stage navigation, ion beam drift correction, milling rates data base
- **Rocking Stage** Multi-directional milling for curtaining reduction, Live SEM imaging for process monitoring, end-point detection
- **Flood gun** Charge neutralisation for reducing charging effects that damage the sample
- **Gas injection system** Delivering of gas chemistry for enhancing milling rates

Ion current	Features	Applications
50 nA 10 nA	▪ High current ▪ Ultra-high speed milling rates ▪ Large spot size	Rough milling for: ▪ Cross-sectioning ▪ Trenches for TEM lamella ▪ Blocks for FIB tomography
1 – 3 nA		▪ Fine polishing: cross-section surfaces, TEM lamellae on the TEM holder, undercutting of lamellae ▪ Horizontal planar delayering
Hundreds of pA 800 pA	▪ Medium spot size ▪ Fast milling rates	▪ Undercutting of lamellae
500 pA 200 pA 100 pA		▪ 3D tomography of volumes < 10^5 µm^3 ▪ Deposition of protective masks (W, Pt) ▪ Lamella attachment to the TEM grid ▪ Final cut of lamellae and attachment to the needle ▪ Polishing of lamellae at different ion accelerating voltages
1 - 50 pA	▪ Very low etching speeds ▪ Small spot size ▪ Ultimate resolution: < 2.5 nm	▪ Very fine polishing of lamellae at low beam energy to reduce ion implantation and amorphous layers ▪ High resolution SI imaging with minimum damage to the sample ▪ Low ion beam energy polishing (≤ 2 kV) for removing amorphous layers in TEM lamellae

Rocking Stage
for curtaining-free polishing

Failure analysis in semiconductor devices relies on high-quality surfaces on cross-sections and lamellae. Finding or identifying possible failures is otherwise very difficult as they can easily hide among surface artefacts. Curtaining are undesirable surface artefacts which appear on surfaces of the samples during FIB milling. Topography, material composition with different etching rates, as well as the characteristic grain and crystal orientation in the sample all contribute to induce curtaining.

The TESCAN Rocking Stage allows multidirectional milling by tilting the sample during FIB etching. Such a technique has proven not only to be effective in eliminating curtaining but also in optimising cross-sectioning tasks and final lamellae polishing. Furthermore, the Rocking Stage allows simultaneous SEM imaging during FIB milling. This enables quality monitoring of the milled surface and guarantees reliable end-point detection. The Rocking Stage has proven to be effective in significantly reducing curtaining artefacts in the following applications.

- **Polishing of cross-sections**

- **Horizontal planar delayering**

is one of the fault isolation techniques used in state-of-the-art technology nodes consisting of top-down layer-by-layer FIB-milling and SEM imaging at low beam energies and low currents. Milling the sample from two different directions has proven to be effective in reducing curtaining effects. The use of the Rocking Stage makes multidirectional milling simple, efficient, and enables larger area delayering in comparison to standard single-direction FIB delayering, Fig. 13.

- **Top-down TEM lamella thinning**

Curtaining effects commonly appear during the thinning process. Even though inverted thinning has proven to help in reducing surface artefacts, it is, however, a time-consuming technique. An alternative and much more efficient technique consists in implementing a two-directional top-down thinning on the Rocking Stage which achieves the same lamella surface quality much faster.

13

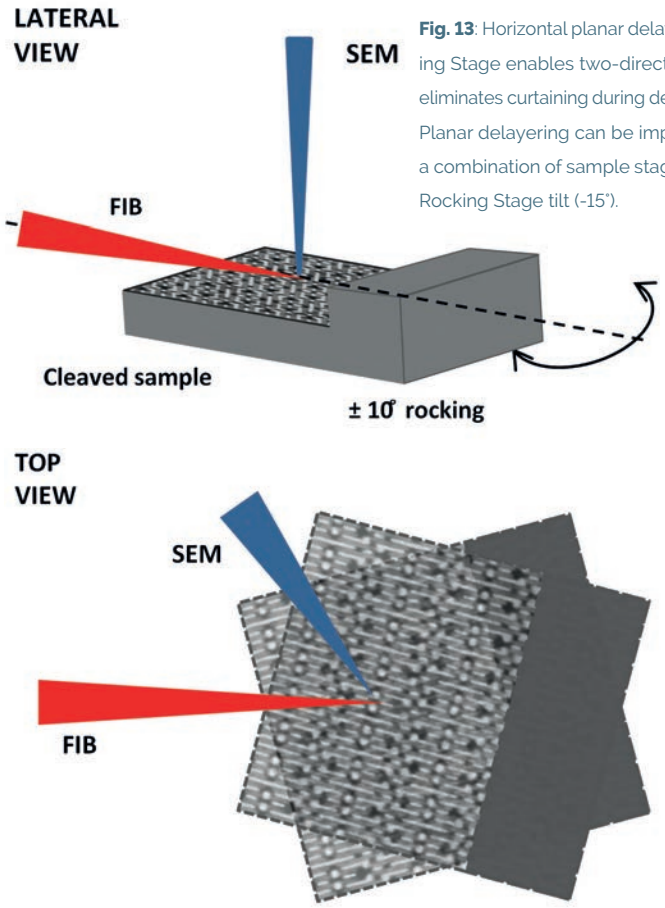

Fig. 13: Horizontal planar delayering on the Rocking Stage enables two-directional milling which eliminates curtaining during delayering processes. Planar delayering can be implemented through a combination of sample stage tilt (-20°) and the Rocking Stage tilt (-15°).

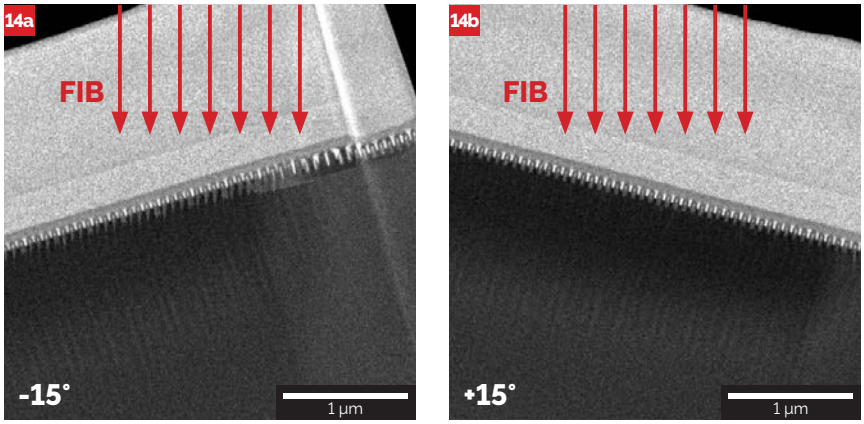

Fig. 14: 14 nm technology node Intel processor. Rocking Stage helps to mitigate curtaining on the TEM lamella by consecutive tilting the sample to **(a)** -15° **(b)** +15° during the lamella thinning.

Speeding up FIB tasks
Optimisation of milling strategies

Optimisation of FIB tasks is possible by taking into account critical factors that have an effect not only on the duration of the process but also on the quality of the milled surface. The milling rate is defined as the volume removed per second, per current unit ($\mu m^3 \cdot nA^{-1} \cdot s^{-1}$). It is different for each material and depends on the incident ion species (mass, energy), the crystallographic structure of the sample, the incidence angle of the ion beam, the dose rate, and also on the amount of re-deposited material during the milling process. In order to maximise milling speeds in cross-sectioning, an optimised milling strategy needs to be implemented to overcome those factors that contribute in slowing down the process.

Material	Milling rate [$\mu m^3/nA \cdot s$]
Si	0.292
Fe	0.674
Cu	1.110
Ag	2.050
Au	2.840

Ga+ FIB milling rates for different materials at 30 keV.

15

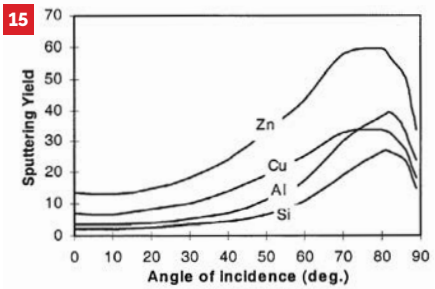

Fig. 15: Dependence of milling yield on the beam incidence angle (respect to the normal to the sample surface) for different materials.

Influence of redeposition

During the milling process, an amount of the sputtered material is redeposited around the milled point. Redeposition is another factor that contributes to decreased milling rates and also affects the aspect ratio of milled structures. Redeposition typically affects the shape especially for very deep trenches, where the escape path is longer. Furthermore, the redeposited material can also be an obstacle for obtaining a clear SEM view of the cross-section.

Influence of the beam incidence angle

The influence of the incidence angle on the milling speed is a well-known effect. For most materials, the maximum milling yield on a free edge occurs when the angle of incidence of the ion beam is about 80° (measured with respect to the normal to the milled surface). This can be up to 5 times higher than that of a normal incidence (0°). The angle of incidence (and milling speed) during milling process changes locally increasing as one moves along the profile line of the milled surface, and so does the milling speed. TESCAN DrawBeam takes this effect into account and optimises the scanning strategy during cross-sectioning by keeping the angle of beam incidence close to that of maximum yield.

16a

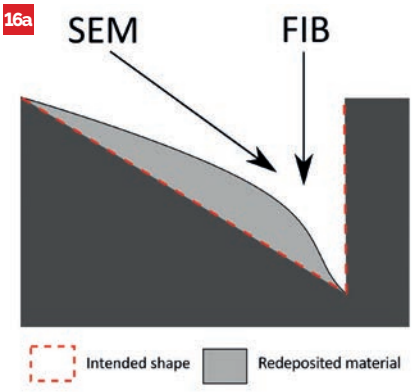

16b

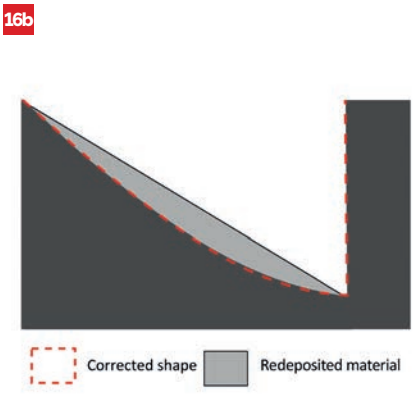

Fig. 16: Shape correction for eliminating redeposition artefacts **(a)** Milling without shape correction **(b)** Milling with shape correction strategy.

17 18 19

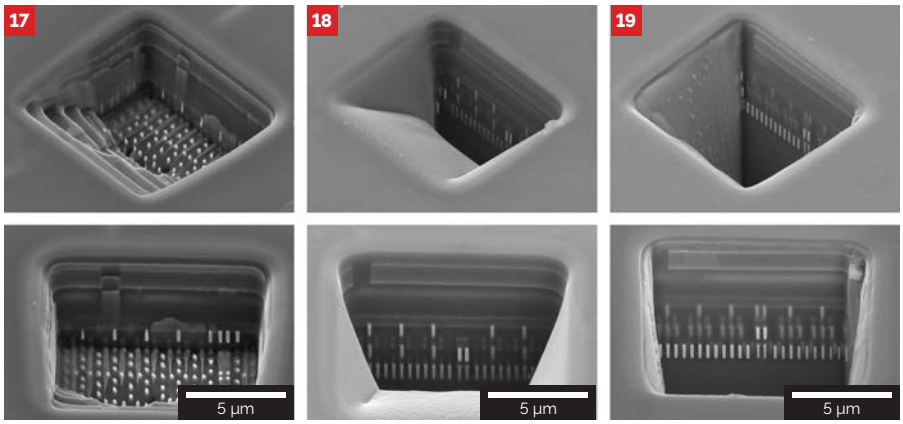

Fig. 17-19: Comparison of different approaches to cross-sectioning. **(17)** Basic top-down staircase scanning strategy showing low depth. **(18)** Single-pass scanning strategy without any optimisation shows increased depth but high redeposition that interferes with SEM imaging. **(19)** Fully optimised strategy showing the highest depth and no redeposition artefacts.

Scanning pattern approaches, based on single or multiple passes, have been implemented in order to deal with redeposition but they result in either low depths or increased depth but high redeposition. The TESCAN DrawBeam software resolves redeposition problems by applying a correction during milling in order to obtain a flat slope at the fastest milling speed. The total depth can be up to 2.5 times deeper and 2.5 faster compared to the scanning strategies mentioned above.

Optimise and maximise throughput in all FIB-SEM applications

Enhance the capabilities and get maximum control in all your FIB-SEM applications with dedicated TESCAN software modules aimed at helping conduct advanced tasks such as milling, material deposition, nanofabrication, etc. All in an easy and simplified way while enabling the automation of different processes.

DrawBeam

is a powerful software for advanced patterning in FIB-SEM lithographic applications such as deposition of protective masks for cross-sectioning or lamellae preparation, electron beam lithography (EBL), and focused ion beam induced deposition (FIBID). DrawBeam enables multi-layer tasks with different processing mode settings (etching/deposition) for each layer. DrawBeam contains a built-in material database, performs slope correction in order to prevent redeposition artefacts and provides precise endpoint detection while making live imaging during milling possible. All features designed to optimise FIB milling.

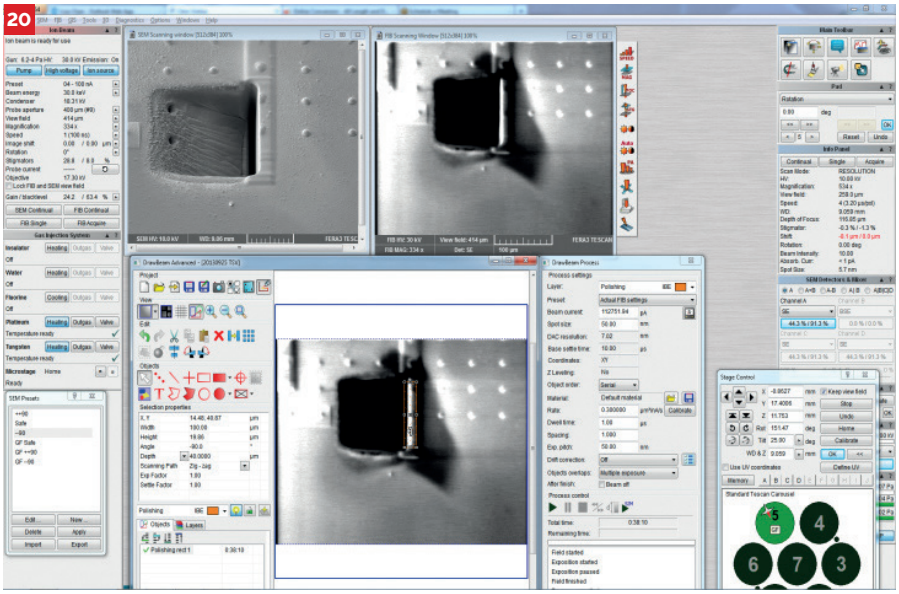

3D Tomography

is a dedicated software for performing FIB-SEM tomography and subsequent 3D reconstructions from collected data. Different visualisation methods are available and data post-processing is possible.

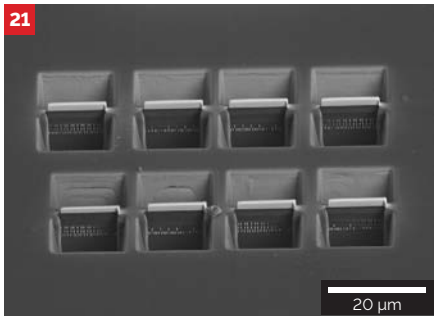

AutoSlicer

enables automation of FIB-SEM operations such as serial cross-sectioning and lamellae preparation or other objects defined at multiple locations. Overnight and unattended operations are possible.

Synopsys Avalon™

Synopsys is a correlative microscopy module for semiconductor applications which includes the Avalon™ software tool for CAD navigation, circuit edit and failure analysis in semiconductors. This software is capable of reading and displaying the physical schematics and layout of a device such as an integrated circuit or a lithographic pattern. The CAD layout is displayed on top of the SEM/FIB image using the DrawBeam software as an interface. Avalon™ is an indispensable tool for electron/ion lithography applications and for all FIB applications such as modification of the sample either for the purposes of prototyping and circuit editing.

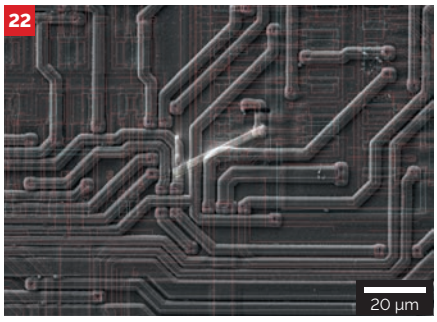

CORAL: Correlative microscopy for life sciences applications

CORAL module allows correlation of data from light microscopy with that from FIB-SEM systems. It works in synergy with the DrawBeam FIB control software platform, where users can create structures directly in the DrawBeam environment.

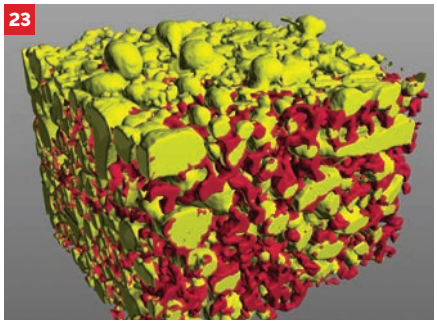

Fig.: (20) Creating a cross-sectioning task in DrawBeam. **(21)** Automatic preparation of site-specific lamellae with AutoSlicer. **(22)** Synopsys Avalon™ enables live overlay of FIB image with CAD design data for precise navigation on an integrated circuit. **(23)** The 3D Tomography software is used for performing 3D sample reconstructions.

Applications

Semiconductors

- **Ultra-fine thinning of TEM lamellae** to thicknesses of less than 15 nm for failure analysis in ≤ 14 nm technology nodes
- **Failure analysis in 3D integrated circuits** by means of planar delayering
- **Prototyping and circuit edit** in multi-layered 3D integrated circuits
- **Imaging of beam-sensitive structures** such as transistor layers, photoresists at low beam energies
- **Ultra-high resolution FIB-SEM tomographies** for unique structural 3D microanalysis
- **In-situ analysis of TEM lamellae** by means of transmitted electrons (STEM) or elemental analysis (EDX, transmission-mode EBSD) at sub-nanometre resolution
- **Inspection and analysis of 6", 8" and 12" wafers**
- **Undistorted high resolution EBSD**
- Enables pioneering accuracy in prototyping, ion beam lithography (IBL), failure analysis of integrated circuits and thin-layer measurement
- **Milling or depositing small specific structures,** benefits of combining FIB with Electron Beam Lithography (EBL)

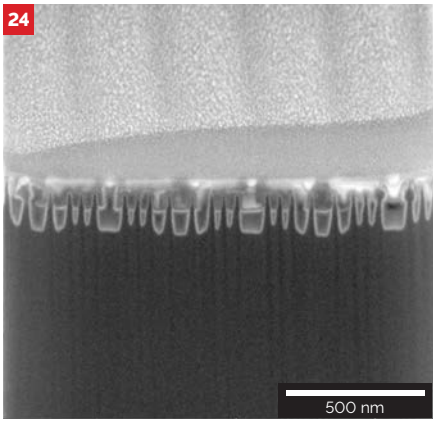

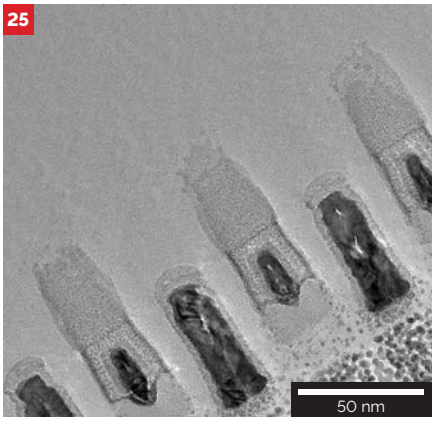

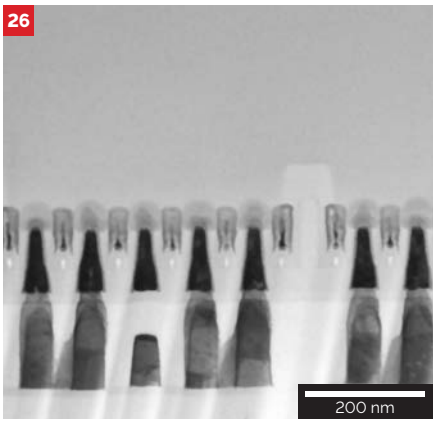

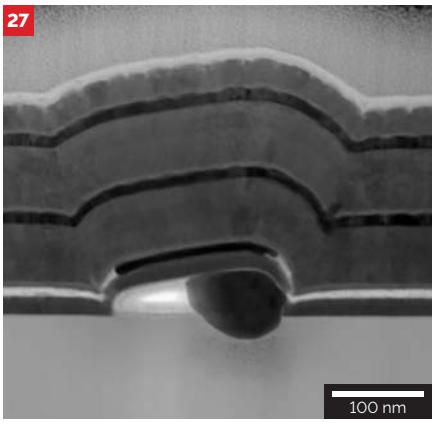

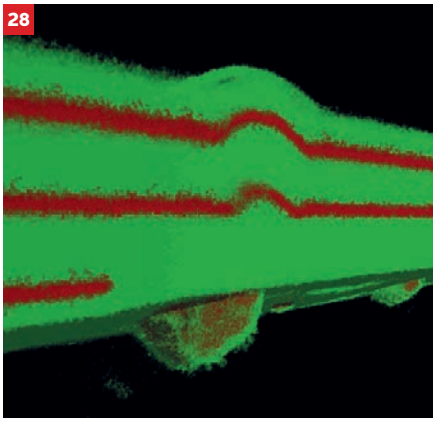

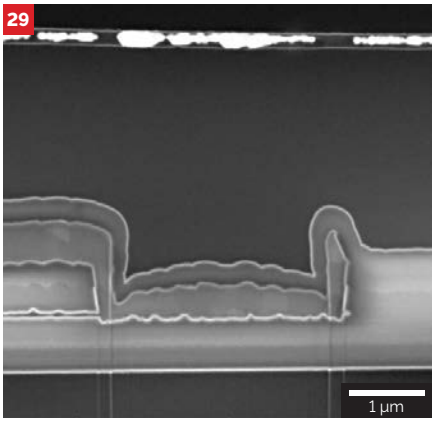

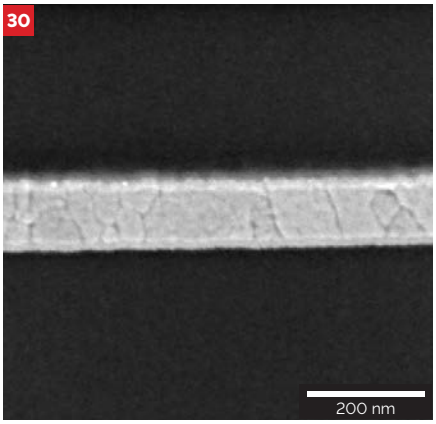

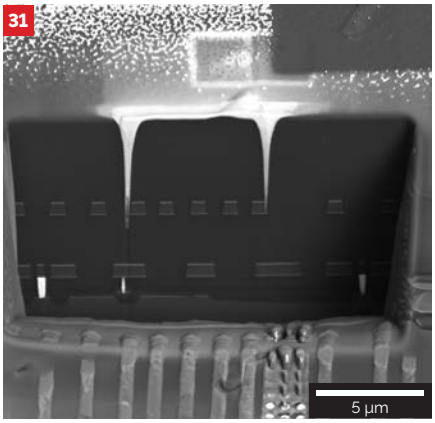

Fig.: (24-25) Failure analysis in a 14 nm technology node. **(24)** Ultra-thin lamella preparation: side view (Fin-cut) of lamella during thinning. The final lamella was prepared just in the middle of a single fin (thickness of < 20 nm). **(25)** A TEM image of a lamella (Gate-cut) prepared by the inverted thinning technique which significantly reduces curtaining. **(26)** A 30 keV STEM-BF image of a lamella from a 22 nm technology node. **(27)** A TEM lamella extracted from a multilayered optical disk for defect examination imaged at 30 keV with the STEM-BF detector. **(28)** A 3nm voxel-size BSE tomography of an optical coating for defect analysis. **(29-30)** OLED display layers quality inspection requires high magnification imaging at low energies. **(29)** Underfilled layer at the top. **(30)** Well-filled layer. **(31)** Circuit editing in a multi-layer microelectronic device through metal vias deposition.

Materials Science

- **Imaging of non-conductive materials** such as ceramics, polymers, glass
- **Characterisation of nanomaterials** such as nanotubes and nanorings
- **Fatigue and crack formation analysis** in metals and alloys
- **Fabrication of nanostructures** such as nanodisks, contacts or hall probes by means of electron beam lithography or focused ion beam induced deposition
- **Imaging of magnetic samples**
- **Preparation of spintronic structures** for the purposes of domain wall motion in magnetic materials and studies on magnetisation dynamics
- **Distinguishing isotopes or species** with similar nominal mass by means of TOF-SIMS analysis
- **Analysis of Li-ion electrodes** by means of TOF-SIMS
- **High-resolution FIB-SEM tomographies** to characterise materials by means of elemental distributions, phases and crystal orientation
- **Corrosion growth studies** by means of secondary ion imaging
- **TEM lamella preparation**

Fig.: (32) A TEM lamella of a MgB_2 sample imaged at 30 keV with the HADF R-STEM detector in the BF mode. **(33)** GaN nanorods imaged at 800 eV with the LE-BSE detector. **(34)** FIB lithography on an Au/Si sample. The widths of the patterned lines are 58 nm and 63 nm. **(35)** A cross-section to evaluate the edge quality in a matrix of holes (diameter of 800 nm in this case) prepared by FIB. The holes were etched through a TiO_2 layer on a resonant crystal substrate. **(36)** 3D reconstructions of Li-ion battery electrodes at different cycling stages. **(37)** A 3D BSE reconstruction showing corrosion growing through Cr plating on steel. **(38-39)** Silicon substrate with nanocrystalline diamonds with Si vacancies (photoluminiscent centres) imaged at 2 keV. **(38)** With the In-Beam SE detector to highlight the topography of the crystallographic facets. **(39)** With the Mid-Angle BSE detector to distinguish between diamond and silicon and provide topographical information.

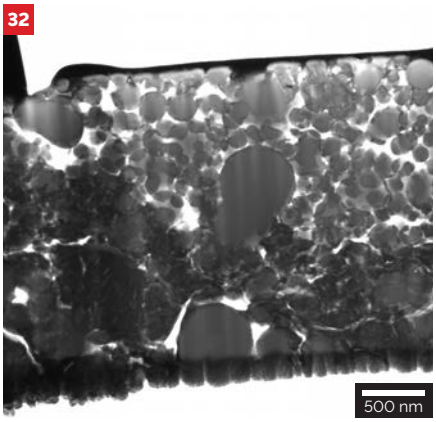

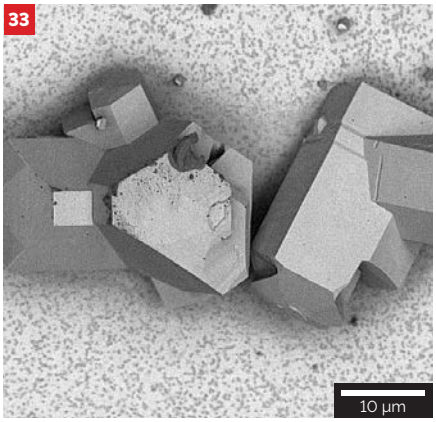

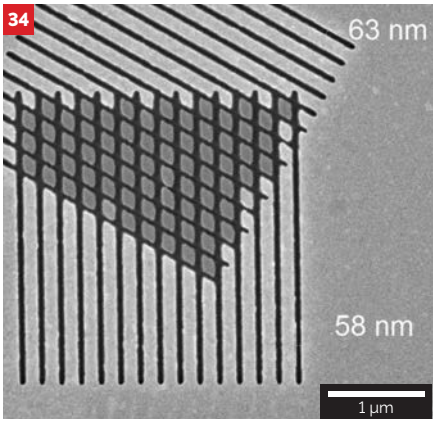

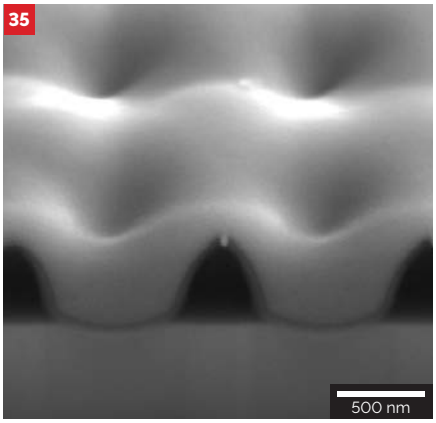

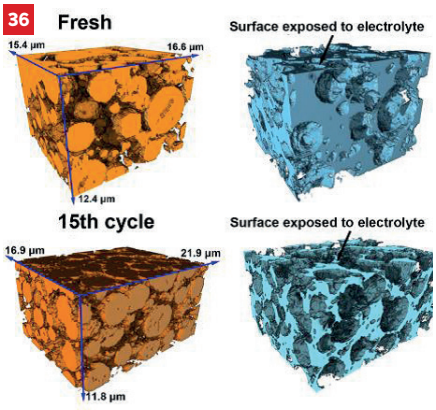

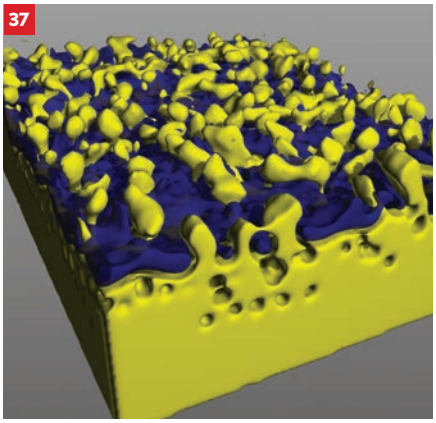

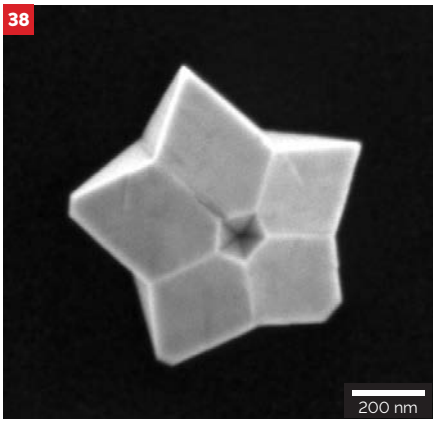

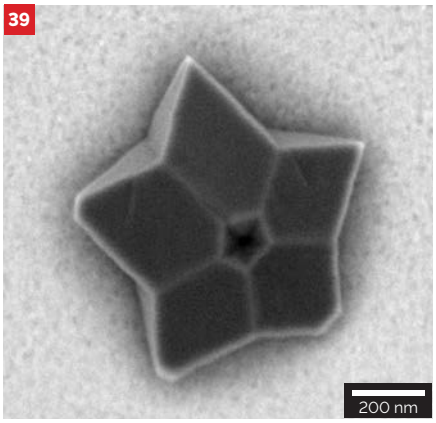

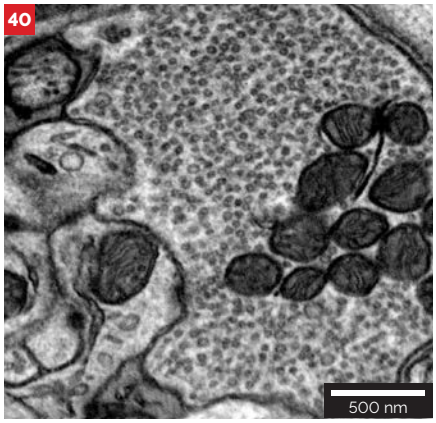

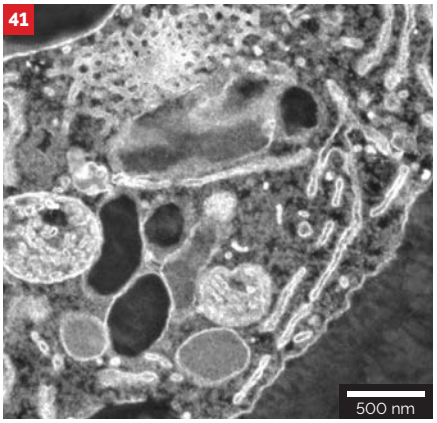

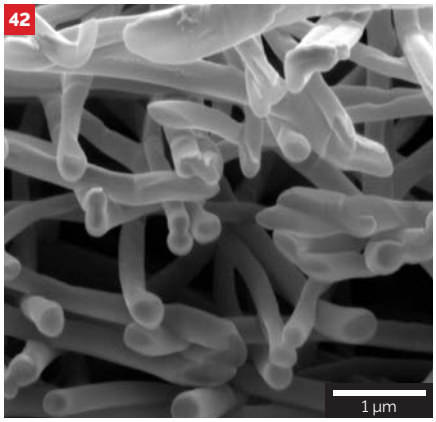

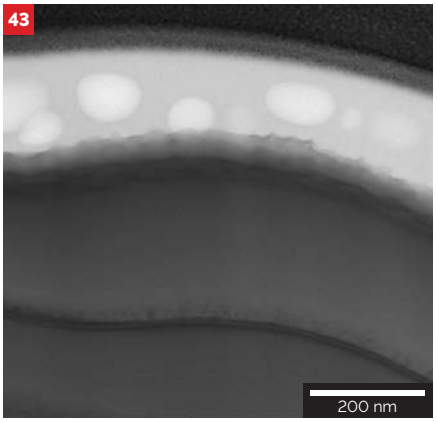

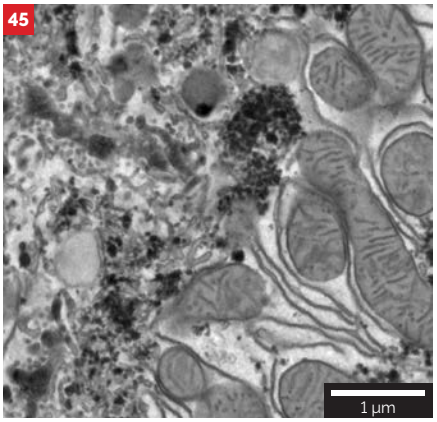

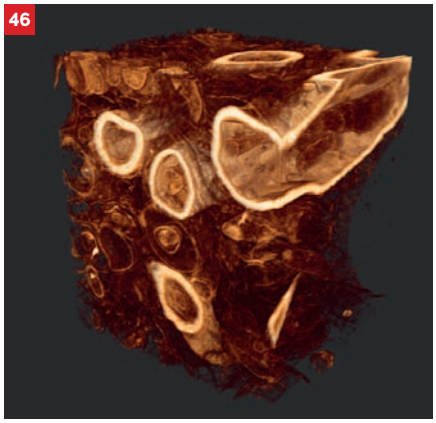

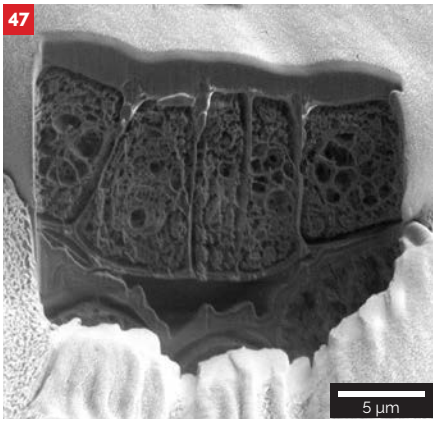

Life Sciences

- **Observation of biological specimens** in their uncoated state at low electron beam energies
- **High-resolution FIB tomography** of highly localised zones for unique 3D structural information of specimens such as resin-embedded animal or vegetal tissue and cells
- **Preparation of thin TEM lamella** of animal and plant tissue for ultra-structural sample analysis
- **In-situ TEM lamella observation** at sub-nanometre resolution
- **High-resolution surface elemental analysis** by means of TOF-SIMS
- **Investigation of cell morphology**, development of biocompatible materials, tissue engineering, microbiology
- **Variable pressure modes** and cryo-techniques for imaging delicate samples
- Correlative light-electron microscopy
- **Cryo-FIB-SEM analysis** of fully hydrated biological specimens

Fig.: (40) Mouse brain tissue stained and embedded in epoxy resin imaged at 3 keV with the LE-BSE detector. **(41)** Resin-embedded barley root section imaged at uncoated at 5 keV with the LE-BSE detector. **(42)** Cross-section in soft polymer nanofibers for their characterisation imaged at 5 keV with the In-Beam SE detector. **(43)** A lamella from a peptide imaged at 30 keV with the STEM detector in the BF mode. **(44)** A high resolution FIB-SEM tomography of resin-embedded yeast. A volume of 10 × 10 × 10 µm^3 was milled with Ga FIB source at 300 pA and with a voxel size of 15 nm. **(45)** Stained mouse liver imaged at 4 keV with the Mid-Angle BSE detector which is ideal for observation of stained biological samples to explore internal tissue structures. **(46)** A 3D BSE reconstruction of mouse cerebellum tissue. A volume of 6.5 × 6.6 × 5.7 µm^3 was milled with Ga FIB source at 300 pA and a voxel size of 10 nm. **(47)** A cross-section in a cryo-frozen leaf surface.

Fabrication of micro- and nano-structures by selective etching of silicon

Selective etching is a technique widely used for local surface modification of different materials. This technique is mainly used in the semiconductor industry for the production of various electrical circuits, photovoltaic cells, etc. Selective etching consists in the application of an etchant and an etchant protective mask. There are two types of selective etching processes, wet and dry etching. A suitable chemical solution (etchant) such as an oxidiser or acid is used for selective wet etching while a beam of energetic ions or reactive plasma is applied for selective dry etching. The etching mask, which is sufficiently resistant to the etchant, is fabricated first by means of a lithographic method.

Selective (local) etching of a substrate material is usually controlled by the etching mask, which is deposited on the substrate surface. The specific mask and etching method determine the quality and properties of the created micro- and nano-structures. In the case of anisotropic etching, the etching rates are different in each direction, and the geometric shapes of the etched structures also depend on the mask orientation due to the substrate surface. An example of anisotropic etching is the case observed in single crystal silicon immersed in a hydroxide solution. The masks can be easily designed with the DrawBeam patterning module and then be prepared by electron beam lithography (EBL) or focused ion beam induced deposition (FIBID).

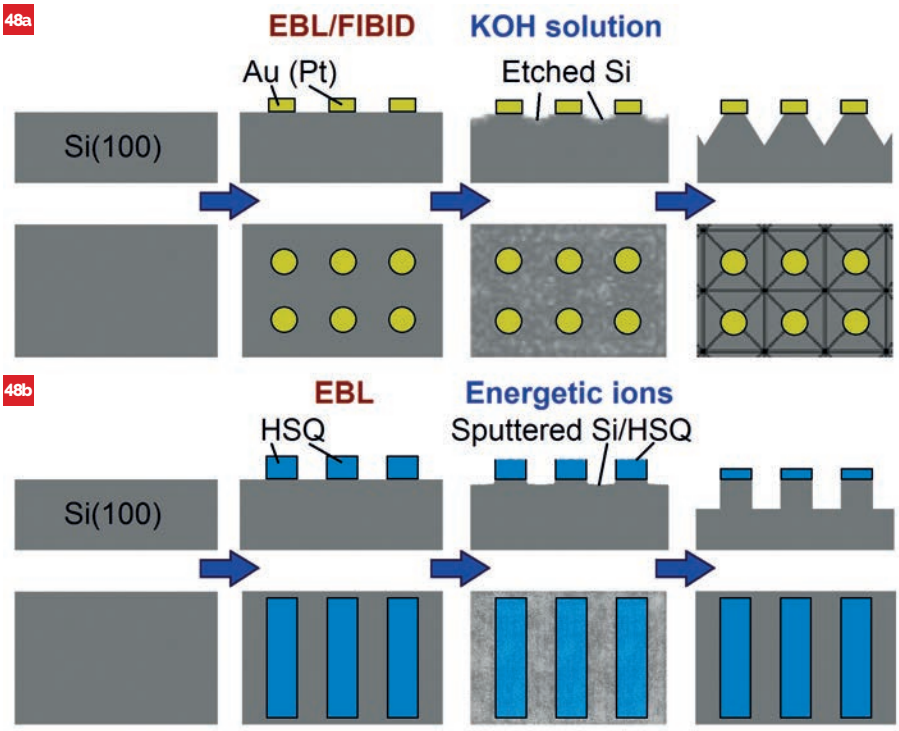

▲ **Fig. 48:** Schematic of micro- and nano-structures fabrication by selective: **(a)** wet etching of Si(100) with a metal mask prepared by EBL or FIBID (a matrix of circles), **(b)** dry etching of the same type substrate with a HSQ resist mask (rectangles).

■ Experimental Conditions

The defined sub-micron structures were fabricated by means of either wet or dry etching of single-crystal silicon with (100) crystallographic orientation and a native SiO_2 layer doped with phosphorous. A 30% KOH water solution kept at a temperature of (50 ± 1) °C was used for wet etching, a process which took several minutes to be completed. The etching rate (in the vertical direction) was 0.22 µm/min under these conditions.

The applied etching masks were prepared by relevant lithographic methods and consisted of the following:

1. Deposition of a 30 (60) nm-thick Au layer with a Ti adhesion layer (3 nm) by means of EBL.
2. Deposition of a Pt layer by means of FIBID.

The whole (wet etching) micro- and nano-fabrication process is illustrated in Fig. 48a. Dry etching was performed by means of ion sputtering at UHV conditions. The kinetic energy of argon ions was adjusted in the range of 50-600 eV. The etching rate of silicon was in the range of a few to several tens of nm/min. The masks were prepared by EBL and consisted of hydrogen-silsesquioxane (HSQ) – a negative EBL resist. The dry etching workflow is shown in Fig. 48b.

Essential Lithography Kit

■ **DrawBeam Advanced**
for creating complex nanopatterning tasks in ion or electron beam lithography applications.

■ **Electrostatic Beam Blanker**
for controlling the beam to produce the required scanning pattern.

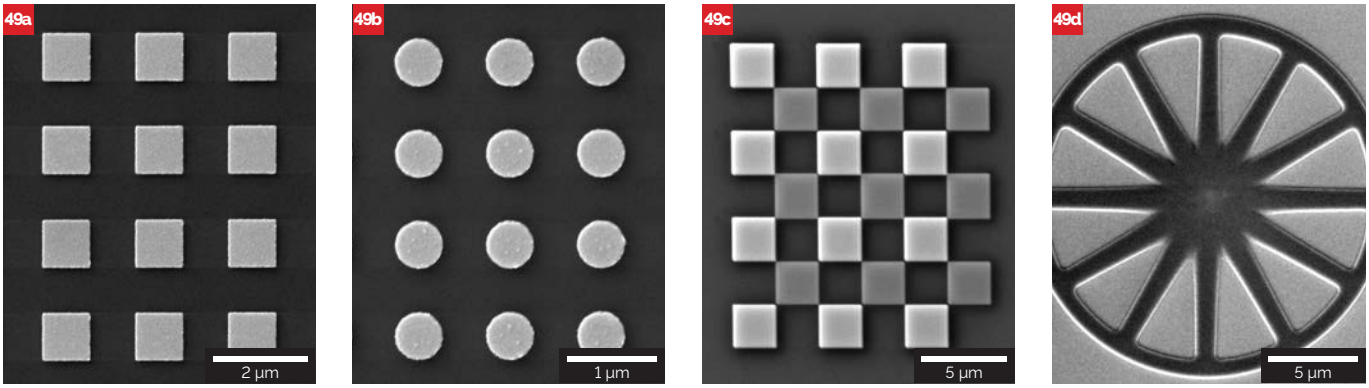

▲ **Fig. 49:** SEM imaging of etching masks (before the etching) consisting of: **a), b)** gold (EBL; a matrix of squares, circles), **c)** platinum (FIBID; a checkerboard pattern) and **d)** HSQ (EBL; a wheel).

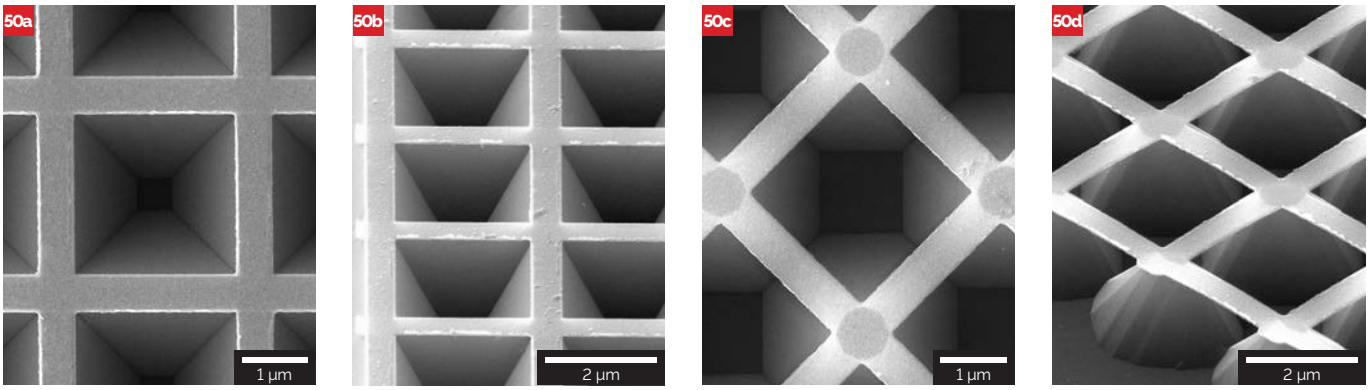

▲ **Fig. 50:** Representation of the level of mask underetching and anisotropic behavior of silicon during the etching in KOH; the angle indicates the rotation of the mask due to the Si(100) wafer (SEM imaging with the sample tilted by (from left) 0°, 55°, 0° and 55°).

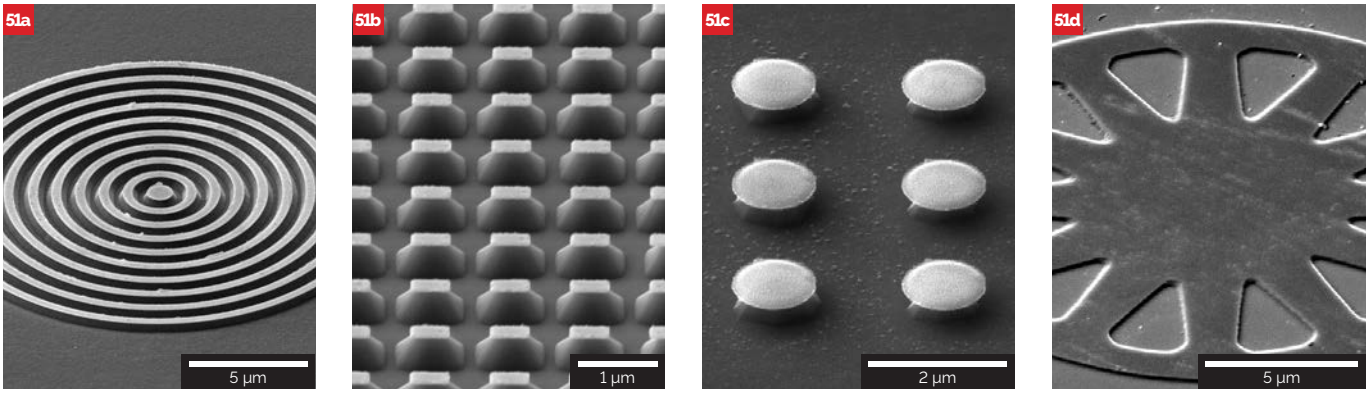

▲ **Fig. 51:** Examples of selective wet etching of silicon with **a), b)** EBL gold mask or **c)** FIBID platinum mask and dry etching of the same substrate type after **d)** HSQ resist mask removal by HF acid (SEM imaging with the sample tilted by 55°).

Results

The fabrication of micro- and nano-structures with different shapes was successfully achieved by means of wet or dry etching, using metal or resist masks (see Fig. 49). The anisotropic properties of Si(100) and, especially the influence of the mask orientation due to the substrate surface, were studied in the case of wet etching in KOH water solution (see Fig. 50). The level of mask underetching was also investigated. The properties of ion sputtering and HSQ mask selectivity (about 0.7) in the case of dry etching were studied. The quality of all fabricated structures was monitored by SEM (see Fig. 51 with etched structures). The lithographic processes were controlled by the DrawBeam software which enabled the design and drawing of different patterns as well as made it possible to work with them in several layers.

Acknowledgements

The work presented in this section was supported by the Technology Agency of the Czech Republic in the frame of the AMISPEC (TE01020233) project.

GAIA3 chamber configurations

XM/GM chambers

The XM/GM chambers are equipped with a compucentric fully motorised specimen stage and their optimised geometry allow multiple detectors to be installed. The chambers can be configured to operate in either high vacuum (XMH/GMH), or under variable pressure (XMU/GMU) - a feature which extends their operations to low vacuum. The XMH/GMH chambers allow imaging of conductive specimens under high-vacuum conditions while the XMU/GMU chambers enable imaging of uncoated non-conductive samples under low-vacuum conditions.

Extended XM and GM chambers

The volume capabilities of the standard XM and GM chambers can be further extended by means of special frontal chamber frames. Larger analytical chambers mean a wider range of applications in science and technology. For instance, such extended chambers offer a concrete solution for the semiconductor industry and fabs as they make the inspection of large wafers possible. The extended XM chamber with a modified Y-axis and an extension frame allows the GAIA3 system to perform SEM inspection as well as FIB micromachining at any location of 6" and 8" wafers. In addition to that, the extended GM chamber also allows SEM inspection of 12" wafers.

Standard Chambers	XM Chamber	GM Chamber
Internal size	290 mm (W) × 340 mm (D)	340 mm (W) × 315 mm (D)
Door	290 mm (W) × 322 mm (H)	340 mm (W) × 320 mm (H)
Maximum specimen height (in mm)	96 (with rotation stage) 137 (without rotation stage)	96 (with rotation stage) 137 (without rotation stage)
Number of ports	12+	20+
Chamber suspension	Integrated active vibration isolation system	Integrated active vibration isolation system

	Specimen Stage in XM Chamber	Specimen Stage in GM Chamber
Type	Compucentric fully motorised	Compucentric fully motorised
Movements (in mm)	X = 130 (-50 to +80) Y = 130 (-65 to +65) Z = 90	X = 130 (-65 to +65) Y = 130 (-65 to +65) Z = 90
Rotation	360° continuous	360° continuous
Tilt	-30° to +90°	-60° to +90°

Vacuum system

Chamber vacuum	High vacuum mode: < 9 × 10^{-3} Pa* Low vacuum mode: 7 – 500 Pa**
SEM gun vacuum	< 3 × 10^{-7} Pa
FIB gun vacuum	< 5 × 10^{-6} Pa
Pumping time after specimen exchange	< 3.5 minutes

*Pressure < 5 × 10^{-4} Pa can be displayed with an optional WRG vacuum gauge (on request)
**With a low vacuum aperture inserted

Software extensions:

Analysis & Measurement	☑
Histogram	☑
Image Processing	☑
3D Scanning	☑
Hardness	☑
Multi Image Calibrator	☑
Object Area	☑
Switch-Off Timer	☑
Tolerance	☑
X-Positioner	☑
Live Video	☑
DrawBeam Basic	☑
EasySEM™	☑
Particles Basic	☐
Particles Advanced	☐
Sample Observer	☐
Image Snapper	☐
DrawBeam Advanced	☐
TESCAN TRACE GSR	☐
3D Metrology (MeX)	☐
3D Tomography	☐
3D Tomography Advanced	☐
System Examiner	☐
Cell Counter	☐
AutoSlicer	☐
Coral (Correlative microscopy module for Life Sciences)	☐
SYNOPSYS Avalon™ (Correlative microscopy module for semiconductor applications)	☐

☑ standard, ☐ option, ⊘ not available

Specifications

Electron Optics

Electron Gun	High brightness Schottky emitter
Resolution	
Standard mode In-Beam SE	0.7 nm at 15 keV 1.4 nm at 1 keV 1.7 nm at 500 eV
Beam Deceleration Mode (option)	1.0 nm at 1 keV - SE (BDM) 1.2 nm at 200 eV - SE (BDM)
STEM detector (option)	0.7 nm at 30 keV
In-Beam LE-BSE	1.6 nm at 15 keV
Low Vacuum Mode:	**BSE:** 2 nm at 30 kV in UH Resolution mode **LVSTD:** 3 nm at 30 keV in Analysis mode
Magnification at 30 keV	4 × - 1,000,000 ×
Maximum Field of View:	4.3 mm at $WD_{analytical}$ 5 mm 7.5 mm at WD 30 mm
Electron beam energy:	200 eV to 30 keV / down to 50 eV with BDT option
Probe Current:	2 pA to 400 nA

Ion Optics

Ion column	Cobra
Ion Gun	Ga Liquid Metal Ion Source
Accelerating Voltage	0.5 kV to 30 kV
Probe Current	1 pA to 50 nA
Resolution	< 2.5 nm at 30 keV (at SEM-FIB coincidence point)
Magnification	Minimum 150 × at coincidence point and 10 keV (corresponding to 1 mm field of view), maximum 1,000,000 ×
SEM-FIB coincidence at	WD 5 mm for SEM - WD 12 mm for FIB
SEM-FIB angle	55°

Detectors*

	XMH GMH	XMU GMU
SE Detector	☑	☑
In-Beam SE Detector	☑	☑
Retractable BSE Detector (In-chamber)[1]	☑	☑
Mid-Angle BSE Detector (In-lens)	☑	☑
In-Beam LE-BSE Detector	☑	☑
Beam Deceleration Technology[2]	☐	☐
LE-BSE Detector[1,3]	☐	☐
Low Vacuum Secondary Electron TESCAN Detector (LVSTD)	⊘	☐
Secondary Ion TESCAN detector (SITD)	☐	☐
STEM Detector	☐	☐
HADF R-STEM Detector[1]	☐	☐
CL Detector[1, 4]	☐	☐
Rainbow CL Detector[1, 4]	☐	☐
EBIC	☐	☐
EDX[5]	☐	☐
WDX[5]	☐	☐
EBSD[5]	☐	☐
TOF-SIMS[5]	⊘ / ☐	⊘ / ☐
WiTec Raman (RISE)	⊘ / ☐	⊘ / ☐

[1]Equipped with motorised mechanics. [2]A package containing BDT and decontaminator is also available. [3]LE-BSE with integrated shutter is mandatory for FIB-SEM tomography and recommended for frequent etching. [4]Compact version with manual retraction available (motorised retraction upon request). [5]Fully integrated third party products.

Optional Accessories*

	XMH GMH	XMU GMU
pA Meter	☑	☑
Touch Alarm	☑	☑
IR TV Camera	☑	☑
Peltier Cooling Stage	☐	☐
Beam Blanker for SEM column	☐	☐
Load Lock**	☐	☐
Control Panel	☐	☐
Optical Stage Navigation	☐	☐
Nanomanipulators	☐	☐
Gas Injection System (5 precursors)	☐	☐
MonoGIS	☐	☐
Decontaminator/plasma cleaner	☐	☐
Flood gun	☐	☐
Rocking Stage***	⊘ / ☐	⊘ / ☐

*Possible combinations of optional detectors and other accessories must be discussed with TESCAN
**Manual and motorised options available
***Automated sample loading possible with Load Lock (motorized) only

System Control

Microscope Control	All microscope functions are controlled via keyboard, mouse and trackball and the GaiaTC program based on the Windows™ platform
Scanning speed	From 20 ns to 10 ms per pixel adjustable in steps or continuously
Scanning features	Point & Line Scan, Focus Window – shape, size and position continuously adjustable, Dynamic Focus – in plane or folded plane tilted up to ±70°, Image rotation, Image shift, Tilt compensation, 3D Beam – defined tilting of the scanning around XY axes, Live Stereoscopic Imaging, Other scanning shapes available through the optional DrawBeam software
Image size	16,384 x 16,384 pixels, adjustable separately for live image (in 3 steps) and for stored images (11 steps), selectable square or 4:3 or 2:1 rectangle Large Panorama Image Size: Unlimited (up to storage capacity)
Automatic procedures	In-Flight Beam Tracing™ beam optimization for both electron- and ion-beams, Spot Size and Beam Current Continual, WD (Focus) & Stigmator, Contrast & Brightness, Scanning Speed (according to Signal-Noise Ratio), Gun Heating, Gun Centering, Column Centering, Vacuum Control, Compensation for kV, Look Up Table, Auto-diagnostics, Setup of FIB-SEM intersection point, GIS nozzle positioning and temperature control, Automated FIB as well as SEM emission start
Remote control	Via TCP/ IP, open protocol

Installation requirements

Power	230 V ± 10% / 50 Hz (or 120 V/60 Hz-optional), power 2,300 + 1,000 VA (basic microscope + chiller)
Water cooling	closed cooling circuit (does not require ext. water supply)
Compressed air	600 – 800 kPa (6 – 8 Bars)
Compressed nitrogen for venting	150 – 500 kPa (1.5 – 5 Bars)
Room for installation	min. 4.5 x 3.5 m; minimum door width 1.0 m
Temperature of environment	17 – 24°C with stability better than 2°C with a rate of change 1°C/hour (0.017°C/min)
Relative humidity	< 65%
Background magnetic field	synchronous < 300 nT asynchronous < 100 nT
Vibrations: **For active isolation**	< 10 µm/s below 30 Hz < 20 µm/s above 30 Hz
Acoustic noise	Less than 60 dBC
Altitude	max. 3,000 m above sea level

Footprint of the microscope GAIA3 XM/GM (all dimensions in mm)

* If a fore-vacuum pump and a chiller unit is to be placed in the same room as the microscope (no technical room with sufficient air exchange is available), then the chiller unit and the fore-vacuum pump must be placed in silencer boxes supplied by TESCAN. The silencer boxes are optional.

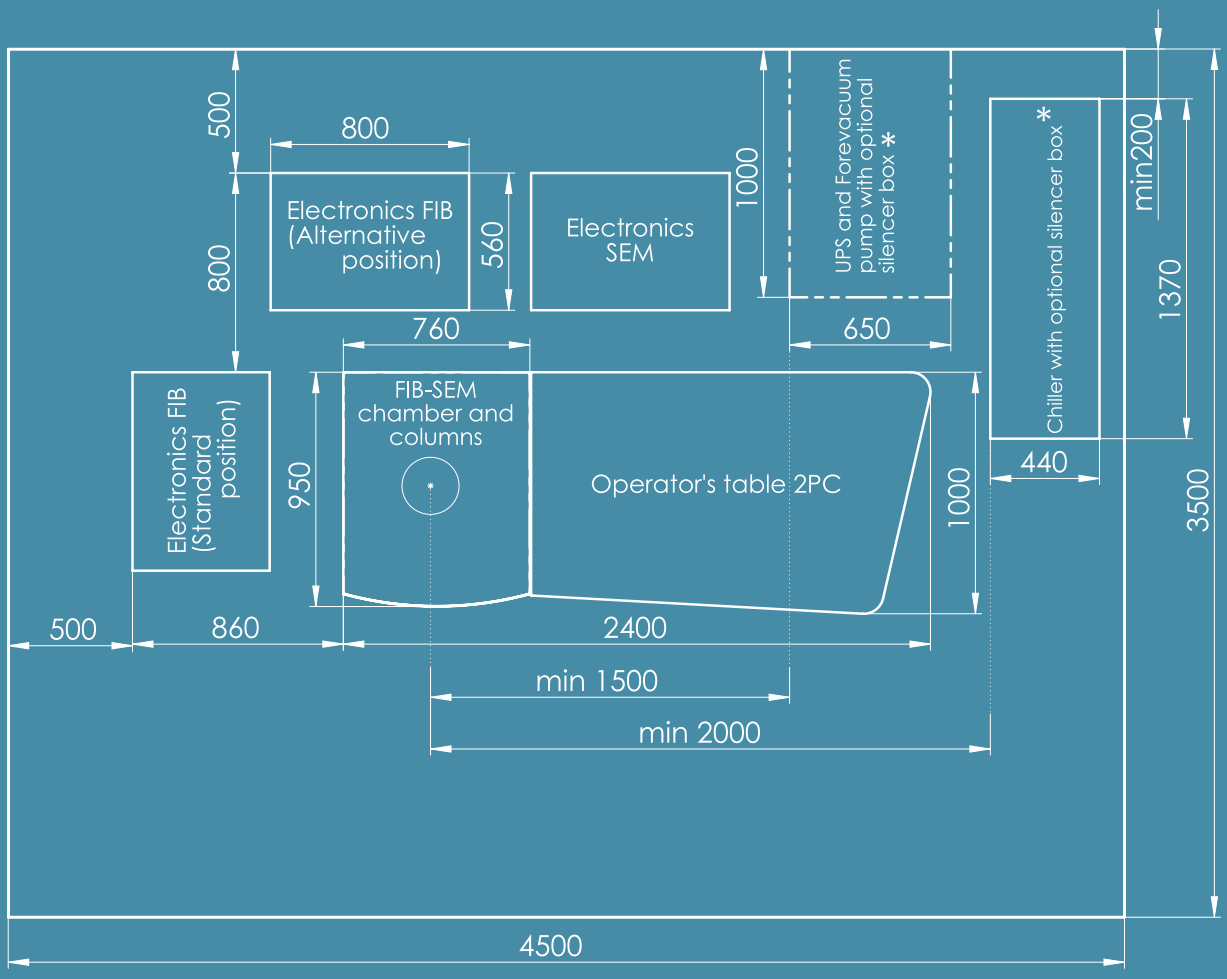

TESCAN
PERFORMANCE IN NANOSPACE

TESCAN ORSAY HOLDING, a. s.
Libušina tř. 21
623 00 Brno - Kohoutovice
Czech Republic
(phone) +420 530 353 411
(email) sales@tescan.cz
(email) marketing@tescan.cz

www.tescan.com